



LJMU Research Online

Al-Kassas, R, Madni, A, Buchanan, C and Shelling, A

pH- sensitive nanoparticles developed and optimized using factorial design for oral delivery of gliclazide

<http://researchonline.ljmu.ac.uk/id/eprint/13126/>

Article

Citation (please note it is advisable to refer to the publisher's version if you intend to cite from this work)

Al-Kassas, R, Madni, A, Buchanan, C and Shelling, A (2021) pH- sensitive nanoparticles developed and optimized using factorial design for oral delivery of gliclazide. Journal of Pharmaceutical Innovation. ISSN 1872-5120

LJMU has developed **LJMU Research Online** for users to access the research output of the University more effectively. Copyright © and Moral Rights for the papers on this site are retained by the individual authors and/or other copyright owners. Users may download and/or print one copy of any article(s) in LJMU Research Online to facilitate their private study or for non-commercial research. You may not engage in further distribution of the material or use it for any profit-making activities or any commercial gain.

The version presented here may differ from the published version or from the version of the record. Please see the repository URL above for details on accessing the published version and note that access may require a subscription.

For more information please contact researchonline@ljmu.ac.uk

<http://researchonline.ljmu.ac.uk/>



LJMU Research Online

Al Kassas, R and Shelling, A

pH- sensitive nanoparticles developed and optimized using factorial design for improving oral absorption of gliclazide

<http://researchonline.ljmu.ac.uk/id/eprint/13126/>

Article

Citation (please note it is advisable to refer to the publisher's version if you intend to cite from this work)

Al Kassas, R and Shelling, A pH- sensitive nanoparticles developed and optimized using factorial design for improving oral absorption of gliclazide. Drug Development and Industrial Pharmacy. ISSN 0095-5183 (Submitted)

LJMU has developed **LJMU Research Online** for users to access the research output of the University more effectively. Copyright © and Moral Rights for the papers on this site are retained by the individual authors and/or other copyright owners. Users may download and/or print one copy of any article(s) in LJMU Research Online to facilitate their private study or for non-commercial research. You may not engage in further distribution of the material or use it for any profit-making activities or any commercial gain.

The version presented here may differ from the published version or from the version of the record. Please see the repository URL above for details on accessing the published version and note that access may require a subscription.

For more information please contact researchonline@ljmu.ac.uk

<http://researchonline.ljmu.ac.uk/>

pH- sensitive nanoparticles developed and optimized using factorial design for oral delivery of gliclazide

Raida Al-Kassas^{1*}, Asadullah Madni², Christina Buchanan³, Andrew N. Shelling⁴

¹School of Pharmacy and Biomolecular Science, Faculty of Science, Liverpool John Moores University, James Parsons Building, Byrom St, Liverpool, L3 3AF, UK.

²Department of Pharmacy, Faculty of Pharmacy & Alternative Medicine, The Islamia University of Bahawalpur, Bahawalpur, 63100, Punjab, Pakistan.

³Department of Molecular Medicine and Pathology, Faculty of Medical and Health Sciences, New Zealand

⁴Department of Obstetrics and Gynaecology, Faculty of Medical and Health Sciences, University of Auckland, Auckland, New Zealand.

*Corresponding author:

Dr Raida Al-Kassas

School of Pharmacy and Biomolecular Science,

Faculty of Science

Liverpool John Moores University,

James Parsons Building, Byrom St,

Liverpool, L3 3AF

UK

pH- sensitive nanoparticles developed and optimized using factorial design for oral delivery of gliclazide

Abstract

Background

Gliclazide is an oral hypoglycaemic agent used for the treatment of non-insulin-dependent diabetes mellitus T2DM. Gliclazide has low solubility in the stomach and poor oral absorption and bioavailability. The pH dependent solubility of gliclazide influences the intra and inter-subject variability.

Purpose

The purpose of this study was to develop, optimize and evaluate pH-sensitive nanoparticles (NPs) based on Eudragit® S100 polymer for oral delivery of gliclazide (GLZ) in an attempt to improve its absorption and bioavailability and to reduce its intra and inter-subject variability.

Methods

Nanoprecipitation technique was used for preparation of GLZ NPs. A 33 full factorial design was applied to study the effect of independent variables (polymer concentration, volume of the organic phase, and stabilizer's concentration) on the mean particle size, zeta potential and the incorporation efficiency of GLZ NPs. The developed optimal formulation was evaluated using various methods including X-ray diffraction (XRD), differential scanning calorimetry (DSC), Fourier transform infrared spectroscopy (FT-IR) and scanning electron microscopy (SEM), drug dissolution and glucose stimulated insulin secretion test.

Results

The analysis of the results revealed transformation of GLZ from crystalline to unstructured form and the absence of any chemical interactions between GLZ and the polymer. The in vitro drug release was dependent on the dissolution behaviour of the polymer. The glucose stimulated insulin secretion test showed incorporation of GLZ into NPs has potentiated its effect on insulin secretion in β cells in presence of (10mM) glucose.

Conclusion

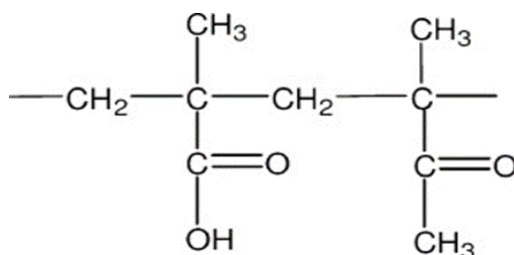
Our study suggests that the optimized NPs have a potential to improve the oral absorption of GLZ.

Keywords: Gliclazide, Eudragit® S100, pH-sensitive nanoparticles, factorial design, insulin secretion test.

1. Introduction

The oral route is the most convenient and commonly used method of drug administration; however, it offers several challenges for drugs especially those with poor solubility and permeability in the gastrointestinal tract (GIT). Conventional solid dosage forms (e.g., tablets and capsules) fail to overcome the obstacles associated with oral delivery of poorly absorbed drugs and often results in bioavailability variability issues. Strategies have been followed to increase drug absorption and bioavailability from the GIT, resulting in development of particulate drug delivery systems [1, 2]. Several studies have reported improved pharmacokinetics profiles and bioavailability of sulfonylureas when delivered by nanoparticulate systems due to enhancements in their solubility [3]. The pH sensitive polymeric nanoparticles, in particular, are an effective formulation for oral delivery of poorly absorbable drugs [4]. The pH sensitive nanoparticles offer several advantages including sustained drug release, ability to increase the specific surface area, and to prolong the residence time of the drug in the gut by interacting with the epithelium surface and enhancing intracellular penetration thus improving drug absorption and bioavailability. Moreover, they can protect drugs against enzymatic degradation and the harsh environment of the stomach by the virtue of their coating [5].

Eudragit® S-100 is a pH sensitive polymer used in pharmaceutical formulation development owing to its unique dissolution behaviour above pH 7.0. It is a copolymer of ethyl acrylate, methyl methacrylate and ethacrylic acid ester with quaternary ammonium compounds (Scheme 1). Eudragit® S100 possesses sustained release properties, plastic deformation, and significant speed sensitivity [6]. Previously, it has been proven that appropriate selection of the pH-sensitive polymer is important for improving the absorption and bioavailability of drugs. Solid dispersion prepared using pH-sensitive Eudragit polymer with the insoluble drug, itraconazole provided prolonged supersaturation along the small intestine for the drug release and improved absorption [7]. Incorporation of a drug in pH sensitive carriers can also avoid precipitation of released drug in the stomach due to solubility issues.



Scheme 1: chemical structure of Eudragit® S100

1
2
3
4
5
6
7
8
9
10
11
12
13
14
15
16
17
18
19
20
21
22
23
24
25
26
27
28
29
30
31
32
33
34
35
36
37
38
39
40
41
42
43
44
45
46
47
48
49
50
51
52
53
54
55
56
57
58
59
60
61
62
63
64
65

Gliclazide (GLZ) is a second generation sulphonylurea oral hypoglycaemic agent used for the treatment of non-insulin-dependent diabetes mellitus T2DM. Gliclazide improves defective insulin secretion and may reverse insulin resistance in T2DM. It is also effective for the treatment of the metabolic defects associated with non-insulin dependent diabetes mellites (NIDDM) and may have the added advantage of potentially slowing the progression of diabetic retinopathy [8]. It is extensively metabolised and has a renal clearance value of 4% of the total drug clearance [9]. The main problem with GLZ is its poor solubility, as it's classified as a BCS-II drug (Drugs with low solubility and high permeability) according to Biopharmaceutical Classification (BCS). Moreover, Gliclazide is a weak acid (pKa 5.8) [10] and has low solubility in the stomach and poor oral absorption and bioavailability. The pH dependent solubility of gliclazide also influences the intra and inter-subject variability. Studies have shown that a single orally administered gliclazide immediate release tablet have low solubility in the stomach that varies the absorption in the intestine [11] and requires a large dose of gliclazide to overcome this problem. For this reason, the recommended gliclazide daily dose ranges from 40mg to 320mg. Erratic absorption, large variations in intra- and inter-subject pharmacokinetics and lack of dose proportionality are all reported problems associated with GLZ, due its poor solubility [12].

Attempts have been made to improve the absorption of GLZ from the GIT and these include preparation of modified release hydrophilic matrix granules [13], monolithic osmotic pump tablets [14], soft gelatin capsule formulations [15], co-grinding of GLZ with carriers [16], inclusion of GLZ in α -cyclodextrin [17], incorporation in alginate beads [18], a self-emulsifying drug delivery system [19], complexating with β -cyclodextrin [20], modified release GLZ biological macromolecules using natural biodegradable polymers [21] and dissolution enhancement of GLZ using in situ micronization [22]. However there are only few studies in the literature reporting the use of pH sensitive nanoparticles for incorporation of GLZ.

Various techniques have been used to prepared nanoparticles. Among these, the nanoprecipitation method has received considerable attention owing to its ability to incorporate water insoluble hydrophobic drugs into nanoparticles [23]. The method involves preparation of organic and aqueous phases separately followed by the addition of one phase to another with the magnetic stirring. Ultracentrifugation and freeze drying are then used to remove the aqueous phase and to produce the nanoparticles powder. To optimize the nanoparticle formulations, several processing conditions need to be investigated and controlled which is time consuming and requires large numbers of experiments

1 to obtain sufficient information about the systems produced. Statistical experimental design including
2 factorial design allows the optimization of nanoparticles using a minimum number of experiments. In
3 addition, relationships and interactions between various variables can be established thus saving time
4 and costs of preparation [24].
5
6

7
8 The aim of this study was to develop pH sensitive nanoparticles optimized by 3³ full factorial design and
9 based on the Eudragit® S100 polymer for oral delivery of GLZ in an attempt to improve its oral
10 absorption and bioavailability and to reduce the intra and inter-subject variability of the drug. The
11 developed optimal formulation was further assessed using fourier-transform infrared spectroscopy
12 (FTIR), differential scanning calorimetry (DSC), X-ray diffraction technique (XRD) and in vitro drug
13 release. The effect of incorporating GLZ into nanoparticles on insulin secretion and the anti-diabetic
14 activities of the developed formulation was evaluated using a cultured mouse pancreatic β cell line,
15 TC6-F7.
16
17
18
19
20
21
22
23

24 25 **2. MATERIALS AND METHODS**

26
27 Gliclazide and tween 60 were purchased from Sigma Aldrich (New Zealand). Eudragit® S-100 was
28 purchased from Evonik Industries (Germany). Potassium dihydrogen phosphate and disodium
29 hydrogen phosphate were purchased from Scharlau (Spain). All other chemicals and reagents used
30 were of AR grade.
31
32
33
34

35 36 **2.1 Experimental Design:**

37
38 A factorial design was followed to optimize production of pH sensitive GLZ nanoparticles (NPs). The
39 effect of polymer concentration, percentage of surfactant and the volume of the organic phase on the
40 physicochemical properties of the prepared nanoparticles were studied. A full 3³ factorial design was
41 applied with a total number of 11 experiments to investigate the influence of the three independent
42 variables: concentration of Eudragit® S100 (X_1), tween 60 (X_2) and acetone (X_3) on the dependent
43 variables: particle size, zeta potential and entrapment efficiency of the nanoparticles. The concentration
44 of GLZ was kept constant throughout the study. For each factor, a range of three levels were
45 investigated at the low, medium and high levels were represented by the signs (-1), (0), and (+1) as
46 shown in Table 1. The levels and the parameters investigated were selected based on previous studies
47 conducted in our laboratory and with consultation with the literature. The data of response parameters
48 were statistically analysed using analysis of variance (ANOVA) at 0.05 level of significance in SPSS
49 version 21. Surface response graphs were plotted by Minitab 15 software.
50
51
52
53
54
55
56
57
58
59
60
61
62
63
64
65

2.2 Formulation of pH- sensitive nanoparticles containing GLZ

pH-sensitive GLZ NPs were prepared by the nanoprecipitation method developed for this study (Fig 1). Briefly, Eudragit® S-100 and GLZ were dissolved in acetone to form the organic phase. The aqueous phase was prepared by dissolving optimized concentrations of tween 60 in distilled water. The organic phase was then added dropwise to tween 60 solution under stirring. The final dispersion was thoroughly mixed at 1200 rpm for 120 minutes. The NPs that resulted were separated by centrifugation, washed with distilled water and freeze-dried (Labconco-7806020, USA). Eleven batches of nanoparticles (F1 to F11) were prepared as per design by varying the concentration of Eudragit® S 100, percentage tween 60 and the volume of acetone in the formulations and maintaining the other experimental conditions constant.

2.3 Particle size and zeta potential

Particle size and Zeta potential were determined using Zetasizer Nano ZS90 (Malvern Instruments Ltd., Malvern, UK). The measurements were performed in triplicate on the nanoparticle suspension in redistilled water at 25 °C.

2.4 Transmission electron microscopy (TEM)

The morphology of the NPs was examined by TEM (Tecnai™ G² Spirit Twin, FEI) with installed Olympus-Soft Imaging Systems Morada camera. Before analysis, the samples were diluted 1:5 and stained with 2% (w/v) phosphotungstic acid for 30 s and placed on copper grids with films for observation.

2.5 Determination of the entrapment efficiency

Freeze dried nanoparticles powder containing GLZ were used. The amount of GLZ entrapped in NPs was determined as follows. NPs containing 8 mg of GLZ were dissolved in 0.5 ml acetone. Then, 10 ml of phosphate buffer pH 7.2 was added to extract GLZ. The mixture was thoroughly mixed for at least 3 hours with constant shaking in a water bath at 37°C. Samples were centrifuged at 20,000rpm and the total amount of the drug in the supernatant was analyzed by a UV-spectrophotometric method (Biochrom Libr S32PC, UK) at a wavelength of 226 nm. The entrapment efficiency (%) of nanoparticles was calculated using the following equation:

$$\text{Entrapment efficiency (\%)} = \frac{\text{Amount of GLZ found in NPs}}{\text{Total amount of GLZ added in NPs}} \times 100$$

2.6 Fourier transformed infrared (FT-IR) spectroscopy

The FT-IR spectra of the pure drug (a), polymer (b), 1:1 GLZ and Eudragit® S100 physical mixture (c) and GLZ NPs formulation (d) were obtained to prove the chemical integrity of the drug in the NPs. The FT-IR spectrum of the samples was recorded in the region of 400 to 4000 cm^{-1} using a FTIR Spectrophotometer (Tensor 37, Brooker-Germany).

2.7 Differential Scanning Calorimetry (DSC)

DSC for the pure gliclazide, Eudragit® S100 polymer, 1:1 physical mixture of GLZ and Eudragit® S100, and GLZ NPs was conducted using a differential scanning calorimeter (Q200 + RCS40, TA instrument, USA). Samples were placed in flat round bottomed aluminium pans and heated to a temperature range of 0 to 300°C at a rate of 10°C per minute with constant purging of nitrogen.

2.8 Powder x-ray diffraction studies

The X-ray diffraction studies of the GLZ, Eudragit® S100, 1:1 physical mixture of GLZ and Eudragit® S100 and the optimized GLZ nanoparticles were performed by a powder X-ray diffractometer (XRD) (Siemens, D5000). XRD patterns were recorded using a graphite monochromatic with copper (Cu) radiation at a voltage of 40 kV and a current of 30 mA at 2θ values.

2.9 *In-vitro* drug release studies and kinetics modelling

In vitro drug release studies of selected optimal GLZ NPs were performed by immersing nanoparticles containing 8mg GLZ in 12 mL phosphate buffer solutions (pH 7.2) in a shaking water bath maintained at 37 °C of speed 100rpm. At regular time intervals, one ml of the dispersion medium was withdrawn and replaced by equal volume of the fresh medium to maintain sink condition. The samples were analysed using UV spectrophotometry at 226 nm and the concentration of GLZ in the samples was calculated using a pre-established standard curve. The *in vitro* drug release studies for GLZ nanoparticles were also conducted in 0.1 M HCl solution of pH (1.2) using the conditions mentioned above. Each experiment was carried out in triplicates.

The *in vitro* drug release data were fitted to different models including zero-order, First-order, Higuchi model and Krosmeier-Peppas model and the equations are illustrated below.

Zero order model $\rightarrow M = M_0 + K_0 t$ [1]

First order model $\rightarrow \log M = \log M_0 - K_1 t / 2.303$ [2]

Higuchi Model $\rightarrow M_t / M_\infty = K_H + t/2$ [3]

Korsmeyer-Peppas Model $\rightarrow M_t / M_\infty = K t^n$ [4]

Where: M_t and M_∞ = Amount of drug release or dissolved drug at time (t), and at equilibrium.

M_0 = Initial amount of drug in solution

K_0 = Zero order rate constant, t = time

K_1 = First order constant

M_t / M_∞ = fraction of drug released at time t.

M_∞ = amount of drug released after an infinite time

K_H = Higuchi rate constant

n = release exponent of Korsmeyer-Peppas power law model

2.10 *In vitro* biological evaluations

a. Preparation of HEPES-buffered krebs ringer buffer (KRB) for β TC6-F7 cells

The HEPES-buffered KRB solution was prepared as detailed in table 6 (supplementary material). The solution was made up to 100 mL or 200 mL in MilliQ water before each experiment.

b. Cell culture

β TC6-F7 cells were cultured in DMEM (Dulbecco's Modified Eagle Medium) supplemented with 15% heat-inactivated horse serum and 2.5% fetal bovine serum (all Invitrogen).

c. Glucose-stimulated insulin secretion test

β TC6-F7 cells [passage 59] were seeded at 10,000 cells per well in 2x24 wells plate. After 48 hrs, culture media was removed, cells washed with 500 μ l KRB, and incubated with 500 μ l of KRB/0.1% BSA for 30min at 37°C. During the preincubation, solutions of 4 mg/L GLZ, empty NPs, 4mg/L GLNPs (preincubated for 3hrs to release gliclazide so that approximately 50% of the drug is released into the solution and 50% remained within the nanoparticles) and 10 mM glucose (all made up in KRB/BSA) were prepared. Equal volumes (250 μ l) each of GLZ solution, empty NPs and GLZ NPs or KRB/BSA control were pipetted into the quadruplicate wells per plate. One plate was incubated with no glucose (250 μ L of KRB/BSA only) and the other with 10mM glucose (250 μ L 20mM glucose in KRB/BSA). Plates were incubated at 37°C for 2 hours. The incubation media was removed from the plate,

centrifuged and analysed for insulin using alphaLISA® (Perkin Elmer) insulin assay after 6 folds dilution in KRB/BSA. A protein assay was also conducted on cell lysate.

3. Results and discussion

The nanoprecipitation technique is a simple and robust method for incorporation of hydrophobic drugs, such as gliclazide, into polymeric nanoparticles. A four steps mechanism takes place during the process of formation of nanoparticles by the nanoprecipitation method: supersaturation, nucleation, growth by condensation, and growth by coagulation [23]. To optimize nanoformulation, various formulation parameters and experimental conditions are usually studied for their effects on the physicochemical properties of the nanoparticles, such as the evaluation of particle size, surface charges and encapsulation efficiency. This requires large number of experiments, which is time consuming and not cost effective. In addition, the interactions between the variables and their effects on the properties of the nanoparticles are not taken into account, which lead to discrepancies between the apparent optimum experimental results and the actual one [25]. Therefore, a full 3³ factorial design was applied for this study, using three independent variables at three levels to overcome the difficulties associated with the conventional method for optimization for a nanoformulation.

3.1. Factorial design analysis for preparation of GLZ NPs

GLZ nanoparticles were prepared following a full 3³ factorial design comprising of 11 experimental runs [24]. The effect of three formulation variables were investigated, these were: concentration of Eudragit® S100 concentration (X_1), % tween 60 (X_2) and volume of acetone (X_3) at three levels (low, medium and high) on the mean particle size (Y_1), zeta potential (Y_2) and entrapment efficiency (Y_3) of the nanoparticles. Table 2 shows the results of the mean particle size, zeta potential and entrapment efficiencies produced from 11 batches. The results show a wide variation in the responses, as the mean particles size varied from 222.233 ± 5.590 to 883.600 ± 539.745 nm (mean \pm SD), whereas zeta potential (ZP) values varied from -1.239 ± 0.865 to -33.899 ± 1.114 mV and percent entrapment efficiency was in the range of 43.478 ± 2.440 to 60.787 ± 0.902 .

Table 3 shows the individual and interactive influence of Eudragit® S100 concentration, % tween 60 in the nanoparticles and volume of acetone on the particle size, as analysed by ANOVA. Particle size is an important attribute owing to its strong effect on the in vivo behaviour of the nanoparticles [26]. Eudragit® S100 concentration significantly affected the size of nanoparticles ($p < 0.05$). Pairwise

1 comparisons (ANOVA) of three levels of Eudragit® S100 showed a significant difference ($p < 0.05$)
2 between lower (100 mg) and higher level (200 mg) and between medium (150 mg) and higher level
3 (200 mg), respectively. Pairwise comparison showed no significant effect of lower (100 mg) with
4 medium level (150 mg) on the size of GLZ nanoparticles. These results suggest that as the
5 concentration of Eudragit® S100 increases as the size of nanoparticles also increases. This can be
6 explained by the higher concentration of polymer has increased the viscosity of the system, and induced
7 particles agglomeration and increased particle size. The increase of the size of nanoparticles may be
8 also increase in thickness and number of layers around GLZ molecules as the polymer concentration
9 increases [27]. A similar observation was reported by others, [28] for GLZ nanoparticles prepared using
10 chitosan polymer. ANOVA results (Table 3) shows a non-significant ($p > 0.05$) effect of the percentage
11 tween 60 at three designated levels on the size of nanoparticles. The effect of acetone at its three levels
12 was also non-significant ($p > 0.05$). On the other hand, neither the interaction of Eudragit® S100 and
13 tween 60, nor the percentage of tween 60 and solvent volumes, showed a significant effect on the size
14 of nanoparticles ($p > 0.05$). The results of the analysis and the surface response (Figure 2 A and B)
15 clearly indicate that the size of nanoparticles is strongly dependent on Eudragit® S100 concentration.
16
17
18
19
20
21
22
23
24
25
26
27
28
29
30

31 Table 4 (ANOVA analysis) and Figure 2 (C and D) surface plots depict the individual and interactive
32 influences of Eudragit® S100 concentration, % tween 60 and volume of acetone on zeta potential (ZP),
33 directly related to the surface charges of the nanoparticles. All three variables significantly ($p < 0.05$)
34 influenced the ZP of nanoparticles. The anionic charges of Eudragit® S 100 and tween 60 resulted in
35 the negative values of ZP and varied with the concentration of polymer used [28]. The ZP, which
36 exemplifies the degree of repulsion between nanoparticles of similar charges, is greatly affected by the
37 composition of the formulation. Theoretically, ZP is the balance between the attractive and repulsive
38 forces that regulate the stability of the colloidal suspension. The suspension remains stable if the
39 repulsive forces are greater than the attractive forces. Nanoparticles with a ZP above $\pm 30\text{mV}$ are stable
40 in suspension due to the repulsion of the surface charges preventing aggregation of the nanoparticles
41 [29]. ZP is an important parameter because the surface charges of colloidal carriers can strongly affect
42 the biodistribution of the drug and stability of the system, and therefore play an important role in its
43 muco-adhesive properties, resulting in prolonging the residence time of the drug at its site of action for
44 absorption. It has been reported that alginate polymer has good muco-adhesion properties due to its
45 anionic nature, due to carboxyl end groups which facilitates its interaction with mucin and the uptake by
46
47
48
49
50
51
52
53
54
55
56
57
58
59
60
61
62
63
64
65

1 Peyer's patches [30-32]. A similar explanation can be applied to Eudragit® S100 (scheme 1) which has
2 an anionic property owing to the many carboxyl end groups in its structure that may assist the adhesion
3 of the particles to mucosal tissues. This together with its unique solubility profile above pH 7 may
4 provide gastro-resistance to the formulations and improves the drug's absorption and bioavailability.
5
6

7
8
9 The effect of volume of acetone, as well as the interaction of the variable x_1x_2 and x_2x_3 on the %
10 entrapment efficiency of nanoparticles was found to be statistically significant ($P < 0.05$) (Table 5 and
11 Figure 2, E &F). Moreover, it was noticed that the % entrapment efficiency increased with increasing
12 with the volume of acetone. This result could be due to the increase of the solubility of GLZ by increasing
13 the volume of the organic phase used, which rendered it more available for encapsulation. Our aim from
14 using the factorial design was to optimize a formulation with appropriate physicochemical properties for
15 oral delivery of GLZ. Ideally, drug delivery system should possess high drug loading as this determine
16 the administration dosage and treatment effects. Moreover, the other attributes such as size, shape,
17 surface chemistry and structure, regulate the nanoparticles behaviours *in vitro* and *in vivo* [33]. For an
18 optimized formulation, the particle size value should be the lowest as possible, irrespective of the
19 administration route [24]. Thus, based on this and from the obtained results, our optimal formulation
20 was found to be Formulation number 6 (F6) and was used for further investigation. The TEM photograph
21 of the optimal GLZ nanoparticles (Figure 3) shows that the nanoparticles are spherical and of a size
22 384 nm confirming the size measurement results obtained by the zetasizer.
23
24
25
26
27
28
29
30
31
32
33
34
35
36
37

38 **3.2 Fourier transforms infrared (FT-IR) spectroscopy**

39
40

41 The FTIR spectra of pure GLZ, Eudragit® S100 polymer, 1:1 physical mixture of GLZ and Eudragit®
42 S100 (1:1 PM) and GLZ nanoparticles formulations are shown in Figure 4. The purpose of this
43 experiment was to assure the compatibility between GLZ and the other components of the
44 nanoparticles. The GLZ spectra shows a sharp Carbonyl (C=O) group peak at 1708 cm^{-1} . The carbonyl
45 group peak remained at same position of 1708 cm^{-1} in both the PMs and nanoparticles spectrum
46 however, it appeared shorter in the nanoparticle spectra. This could be attributed to interaction between
47 GLZ and Eudragit® S100. The amino (NH) group peak located at 3271 cm^{-1} in GLZ spectra has shifted
48 to 3265 cm^{-1} in PMs but broadened in the nanoparticle profile. A similar observation was reported for
49 GLZ incorporated into Eudragit® L100 nanospheres by Lo et al., 2003 and was explained by an
50 interaction between GLZ and the encapsulating polymer. The two bands of sulfonyl group, a symmetric
51
52
53
54
55
56
57
58
59
60
61
62
63
64
65

1 stretching peak at 1164 and an asymmetric stretching peak at 1350, characterizes the GLZ spectra.
2 Both of symmetric and asymmetric peaks retained their positions in the nanoparticles, and the physical
3 mixtures of GLZ and Eudragit.
4
5

6
7 In summary, the spectral illustration indicates that there is no difference between the internal structures
8 and conformation of pure GLZ and Eudragit® S100 at the molecular level; hence it is evident that there
9 is no interactions observed between different components employed for preparation of nanoparticles
10
11 Moreover, GLZ NPs FT-IR spectrum analysis showed no significant changes of GLZ and suggested
12 that the molecules of gliclazide might have dispersed completely into the Eudragit® S100 polymeric
13 matrix [3].
14
15
16
17
18
19

20 **3.3 Differential Scanning Calorimetry (DSC)**

21
22
23 DSC is a quick technique to examine the melting endotherm and recrystallization behaviour of a material
24 that has a crystalline structure and to determine if a drug is completely dispersed into a polymeric matrix
25 in the formulation [33, 34]. The DSC thermograms of pure GLZ, Eudragit® S100, 1:1 physical mixture
26 of GLZ and Eudragit® S100 (PMs), and GLZ nanoparticles formulation are shown in Figure 5. In the
27 Eudragit® S100 sample, a glass transition temperature region and an exothermic peak located at 218
28 °C and heat flow of 0.65W/G and a broad shallow peak due to water evaporation were observed. The
29 pure GLZ showed a sharp endothermic peak at 169.32 °C, corresponding to its melting point and heat
30 flow of 2.383 (Watt per gram) (W/G) indicating its crystalline nature. The physical mixture of the drug
31 with as measured by polymer thermogram revealed the presence of GLZ endothermic signal confirming
32 that GLZ crystals still exist in PMs. On the other hand, the GLZ nanoparticle formulation showed a
33 short broad endothermic peak of GLZ at 165°C with a heat flow of 0.591 W/G, which is an evidence of
34 reducing the crystallinity of GLZ in the optimized formulation [35]. This finding will be confirmed by the
35 X-ray diffraction studies.
36
37
38
39
40
41
42
43
44
45
46
47
48
49

50 **3.4 X-ray diffraction (XRD) studies**

51
52
53 The XRD of pure GLZ, Eudragit® S100 polymer, 1:1 physical mixtures of GLZ and Eudragit® S100,
54 and GLZ NPs are shown in Figure 6. The XRD spectra of GLZ shows peaks at the diffraction angles
55 (2θ) of 10.61, 15.12°, 17.65°, 18.41, 22.1, 23.4, 26.5, 28.7.52 °C which are characteristics peaks of
56 GLZ and exhibit its crystallinity. No distinctive diffraction peaks were observed for Eudragit® S100 owing
57
58
59
60
61
62
63
64
65

1
2
3
4
5
6
7
8
9
10
11
12
13
14
15
16
17
18
19
20
21
22
23
24
25
26
27
28
29
30
31
32
33
34
35
36
37
38
39
40
41
42
43
44
45
46
47
48
49
50
51
52
53
54
55
56
57
58
59
60
61
62
63
64
65

to its non-crystalline nature [36]. The 1:1 physical mixture of GLZ and Eudragit® S100 shows the diffraction features of GLZ. However, the pattern of GLZ nanoparticles was significantly different from that of the pure drug and PMs as only a few diffraction bands were observed at 15°, 30° and 52° for GLZ, but with low intensity, and many peaks have disappeared indicating transformation of gliclazide from crystalline to unstructured form in the nanoparticles [37]. The reduction in the crystallinity of the entrapped GLZ in nanoparticle formulations could enhance the solubility, thereby the absorption and the oral bioavailability of GLZ [38,39].

3.5 *In vitro* drug release studies

Eudragit® S100 is a pH-sensitive polymer, which can be used to develop novel drug delivery systems for controlling the drug release in the GIT, thereby enhancing the drug's pharmacokinetics profile. Eudragit® S100 has other beneficial properties that have been considered for the preparation of nanoparticles for GLZ in our study; it is widely used as a pharmaceutical excipient (e.g. enteric coating material), generally regarded as non-toxic, has been approved by FDA for human use, and has advantages in mucosal uptake of the compounds loaded in nanoparticles.

The *in vitro* drug release of the pH sensitive GLZ nanoparticles was studied in 0.1M HCl (pH 1.2) and phosphate buffer (pH 7.2) and the results are shown in Figure 7. As can be seen, the pH environment significantly affected the release profiles of GLZ. In 0.1 M HCl, the release of GLZ was very slow. The cumulative amount of GLZ released gradually reached about 20% as the entrapped drug within the nanoparticles was diffused out over 6 hrs. The release rate of GLZ distinctively increased, as the pH of the dissolution medium changed from 1.2 to 7.4 at which Eudragit® S100 nanoparticles quickly dissolved, achieving 80% of the release amount of the loaded drug within 6 hrs. Eudragit® S100 is an anionic copolymer of methacrylic acid and methyl methacrylate containing free carboxylic and ester groups. It has low permeability and is nearly insoluble in acidic medium owing to the high intermolecular attraction between its molecules. The observed release of GLZ at pH 1.2 could be due to leaching of the drug from the outer surfaces of the nanoparticles. On the other hand, Eudragit® S100 dissolves at above pH 7.0. Dissolution occurs as a result of structural changes of the polymer associated with ionization of the carboxylic functional group. The rapid dissolution and erosion of the Eudragit® S100 polymeric nanoparticles in phosphate buffer pH 7.2 has greatly contributed in facilitating the drug release rate in this medium. These results suggest that the dissolution behaviour of Eudragit® S100 polymer is the major factor controlling the release of the GLZ from the formulation. Indeed, we have

1 employed a pH sensitive polymer which is insoluble in acidic pH (0.1 M HCl) and therefore a minimum
2 amount of GLZ (less than 5%) was released in two hours (the gastric emptying time). However, at the
3
4 physiologic pH of intestine (pH 7.2), GLZ was released in a controlled manner over 6 hrs which may
5
6 improve the *in vivo* behaviour of the drug and consequently enhance its pharmacokinetics profile.
7

8
9 The release data at pH 7.2 were fitted to different kinetic models including zero-order, first-order,
10 Higuchi and Krosmeier-Peppas models. The kinetics models were used to describe different release
11 behaviours of drugs from their formulations. The zero-order model is used for systems where the drug
12 is released slowly, irrespective of the initial drug concentration. In the first-order model, the drug release
13 is directly proportional to the drug concentration incorporated in the delivery system. Hence, the drug
14 concentration decreases with time. On the other hand, Higuchi's model is used where the release
15 mechanism is a pure diffusion process of the drug from the delivery system in the absence of erosion
16 or swelling, assuming the drug is homogenously dispersed in the system. The Krosmeier-Peppas
17 model can be used as a decision parameter between the Higuchi and zero order models. Criteria for
18 selecting the most appropriate model is based on the best fit indicated by the value of coefficient of
19 determination (R^2) closer to 1. On the basis of best fit with the highest correlation coefficient (R^2) value,
20 we have concluded that GLZ nanoparticles follow the Krosmeier-Peppas model. The determined R^2
21 value was found to be 0.9923 and the calculated release exponent [n] was 0.49. The magnitude of the
22 release exponent 'n' suggests that the release mechanism is an anomalous transport or non Fickian
23 diffusion, as the values of the exponent 'n' lies between 0.43 and 0.85, which is related to a combination
24 of both diffusion of the drug and dissolution of the polymer [40].
25
26
27
28
29
30
31
32
33
34
35
36
37
38
39
40

41 **3.6 Glucose-stimulated insulin secretion test**

42
43 Insulin is released by pancreatic β -cells and controls the glucose level in the blood stream when blood
44 sugar concentration rises. Diabetes occurs when the viability and functions of pancreatic β cells
45 decrease relative to peripheral insulin activity. Sulphonylureas are drugs that stimulate insulin release
46 in the absence of glucose, by binding to sulphonylurea receptors [41] Gliclazide belongs to the
47 sulphonylurea family and is known to binds to sulfonylurea receptors in β cells and stimulates insulin
48 release. We investigated the effect of GLZ NPs on insulin secretion from β -cells treated with GLZ
49 standard, empty NPs, GLZ NPs or KRB/BSA control in the presence (10mM) and absence (0mM) of
50 glucose. Figure 8.a&b shows that β TC6-F7 cells in the absence of glucose (0mM) did not exhibit high
51 level of insulin release in formulation investigated. Whereas, high glucose (10mM) caused an
52
53
54
55
56
57
58
59
60
61
62
63
64
65

1 approximately fourfold increase of insulin secretion. There was a clear and significant stimulation of
2 insulin secretion in response to the GLZ standard in the absence of glucose (0mM). On the other hand,
3
4 incorporation of GLZ into nanoparticles potentiated its effect on insulin secretion in β TC6-F7 cells in the
5
6 presence of (10mM) glucose. An important key in cellular delivery is binding of the drug carriers with
7
8 the target cells. It has been previously reported that the nanoparticle size plays a significant role in their
9
10 adhesion to living cells and subsequent interaction [42]. Nanoparticles of about 100–200 nm are
11
12 internalized by receptor-mediated endocytosis, while larger particles are taken up by
13
14 phagocytosis/endocytosis. Our results are in agreement with this hypothesis since the GLZ
15
16 nanoparticles exhibited a particle size above 200nm and may have been internalized with β -cells by an
17
18 endocytosis mechanism [42]. However, multiple factors can affect nanoparticle internalization such as
19
20 cell line dependence, particle size, and surface composition. It has been established that Eudragit®
21
22 S100 possess a bio-adhesive property. Bio-adhesive materials are generally hydrophilic
23
24 macromolecular compounds that contain numerous hydrogen bond forming groups, such as carboxyl,
25
26 hydroxyl, amide and amine groups, and will hydrate and swell when placed in contact with an aqueous
27
28 solution [43]. In our study, the Glucose-Stimulated insulin secretion test has been carried out at pH 7.4
29
30 (Table 6 in the supplementary materials) and Eudragit S100 polymer hydrates and swells at pH above
31
32 7. In this regards, we suggest the entry of the GLZ nanoparticles to β -cells was achieved by their bio-
33
34 adhesive nature in addition to their small size. We speculate the possibility for the increase of insulin
35
36 secretion caused by GLZ nanoparticles in the presence of glucose (10mM) is that the GLZ nanoparticles
37
38 with their bio-adhesive properties and their small size have increased the uptake of nanoparticles by β
39
40 cells, where sulphonyl urea receptors are present, thereby facilitating binding of the GLZ to the receptor.
41
42 Our results confirm that the incorporation of GLZ into Eudragit® S100 nanoparticles retains its original
43
44 biological activity, but also has improved the cellular uptake and binding of GLZ to sulfonylurea
45
46 receptors.

48 **4. Conclusion**

49
50 In this study pH sensitive nanoparticles were developed using factorial design for oral delivery of
51
52 gliclazide. The 3^3 factorial design based on Eudragit® S100 polymer, tween 60 and acetone, as three
53
54 independent variables, has successfully guided formulation optimization of GLZ nanoparticles with
55
56 desirable particle size, surface charges and loading efficiency properties. The in vitro drug release
57
58 studies of the optimized GLZ nanoparticle formulation was dependent on the dissolution behaviour of
59
60
61
62
63
64
65

1 the polymer, but in general, the release was prolonged. Additionally, the formulation components used
2 for nanoparticles were compatible and no interactions were detected as shown by the FTIR, DSC and
3
4 XRD studies. The glucose stimulated insulin secretion test revealed that incorporation of GLZ into pH
5
6 sensitive Eudragit® S 100 nanoparticles has potentiated its effect on insulin secretion in β cells in
7
8 presence of (10mM) glucose.
9

10
11
12
13 **Conflict of interest:**

14 The authors declare no potential conflict of interests.
15
16
17
18
19
20
21
22
23
24
25
26
27
28
29
30
31
32
33
34
35
36
37
38
39
40
41
42
43
44
45
46
47
48
49
50
51
52
53
54
55
56
57
58
59
60
61
62
63
64
65

References

- 1
2
3 [1] Miyata K, Christie RJ, Kataoka K. Polymeric micelles for nano-scale drug delivery. *React Funct. Polym.* 2011; 71: 227-234.
- 4
5 [2] Bennet D, Kim S(Eds.), *Polymer Nanoparticles for Smart Drug Delivery*, InTechOpen, (2014) 257-310.
- 6
7
8 [3] Lo Y, Chen C, Tsai T et al. Comparison of the solubility and dissolution rate between gliclazide solid complex and its nanospheres. *Drug Dev. Ind. Pharm.* 33 (2007) 301–309.
- 9
10 [4] Jog R, Unachukwu K, D. Burgess D. Formulation design space for stable, pH sensitive crystalline nifedipine nanoparticles. *Int. J. Pharm.* 2016; 514: 81-92.
- 11
12 [5] Wang XQ, Zhang Q. pH-sensitive polymeric nanoparticles to improve oral bioavailability of peptide/protein drugs and poorly water-soluble drugs. *Eur. J. Pharm. Biopharm.* 2012,82: 219-229
- 13
14 [6] Tatavarti SA, Francis X, S. Muller S et al. Evaluation of the deformation behavior of binary systems of methacrylic acid copolymers and hydroxypropyl methylcellulose using a compaction simulator *Int. J. Pharm.* 2008, 348: 46–53.
- 15
16 [7] Dave A. Miller, James C. DiNunzio, Wei Yang, James W. McGinity & Robert O. Williams III. Targeted Intestinal Delivery of Supersaturated Itraconazole for Improved Oral Absorption. *Pharmaceutical Research* volume 25, pages1450–1459(2008)
- 17
18 [8] Katharine J, Palmer R, Brogden G. Gliclazide, *Drugs*, 46 (1993) 92-125. doi: 0012-6667/93/0007-0092.
- 19
20 [9] Campbell DB, Lavielle R, Nathan C. The mode of action and clinical pharmacology of gliclazide: a review *Diabetes Res. Clin. Pract.*, 14 (1992) Supplement 2, S21-S36. doi: [http://dx.doi.org/10.1016/0168-8227\(91\)90005-X](http://dx.doi.org/10.1016/0168-8227(91)90005-X).
- 21
22 [10]L. Sambath, A.K. Muthu, M.A. Kumar, K. Phaneendra, Shalini. Physicochemical characterization and in-vitro dissolution behavior of gliclazide–soluplus solid dispersions. *Int. J. Pharm. Pharm. Sci.*, 5 (2) (2013), pp. 204-210
- 23
24 [11] Kilo, C., Dudley, J. & Kalb, B. Evaluation of the efficacy and safety of Diamicron® in non-insulin-dependent diabetic patients. *Diabetes Res. Clin. Pract.* 2, S79–82 (1991).
- 25
26 [12] Desai PP, Date AA, Patravale VB. Overcoming poor oral bioavailability using nanoparticle formulations – opportunities and limitations. *Drug Dis. Today: Technologies.* 2012, 9: e87-e95. doi: <http://dx.doi.org/10.1016/j.ddtec.2011.12.001>.
- 27
28 [13] Harrower A, Gliclazide modified release: From once-daily administration to 24-hour blood glucose control, *Metab. Clin. Exp.* 2000, 49: 7-11. doi: <http://dx.doi.org/10.1053/meta.2000.17823>.
- 29
30 [14] Guan J, Xiang R, Pan Y et al. Design and evaluation of a novel formulation prediction system. *Int. J. Pharm.* 2010, 402: 129-139. doi: <http://dx.doi.org/10.1016/j.ijpharm.2010.09.036>.
- 31
32 [15] Hong SS, Lee SH, Lee J et al. Accelerated oral absorption of gliclazide in human subjects from a soft gelatin capsule containing a PEG 400 suspension of gliclazide. *J. Control Rel.* 1998, 51: 185-192. doi: [http://dx.doi.org/10.1016/S0168-3659\(97\)00167-3](http://dx.doi.org/10.1016/S0168-3659(97)00167-3).
- 33
34 [16] Barzegar-Jalali M, Valizadeh H, Shadbad MS et al. Single non-ionic surfactant based self-nanoemulsifying drug delivery systems: formulation, characterization, cytotoxicity and permeability enhancement study. *Powder Technol.* 2010, 197: 150-158. doi: <http://dx.doi.org/10.1016/j.powtec.2009.09.008>.
- 35
36
37
38
39
40
41
42
43
44
45
46
47
48
49
50
51
52
53
54
55
56
57
58
59
60
61
62
63
64
65

- 1 [17] Arias-Blanco M J, Moyano JR, Perez-Martinez JI et al. Study of the inclusion of gliclazide in α -
2 cyclodextrin. *J. Pharm. Biomed. Anal.* 1998, 18: 275-279. doi: [http://dx.doi.org/10.1016/S0731-](http://dx.doi.org/10.1016/S0731-7085(98)00179-4)
3 7085(98)00179-4.
- 4 [18] Al-Kassas R, Al-Gohary O, Al-Faadhel M. Controlling of systemic absorption of gliclazide through
5 incorporation into alginate beads. *Int. J. Pharm.* 2007, 341: 230-237. doi:
6 <http://dx.doi.org/10.1016/j.ijpharm.2007.03.047>.
- 7 [19] Nipun TS, Ashraful Islam SM. SEDDS of gliclazide: Preparation and characterization by in-vitro,
8 ex-vivo and in-vivo techniques. *Saudi Pharm. J.* doi: <http://dx.doi.org/10.1016/j.jsps.2013.06.001>.
- 9 [20] Özkan Y, Atay T, Dikmen N et al. Improvement of water solubility and in vitro dissolution rate of
10 gliclazide by complexation with β -cyclodextrin. *Pharm. Acta Helv.* 2000, 74: 365-370. doi:
11 [http://dx.doi.org/10.1016/S0031-6865\(99\)00063-1](http://dx.doi.org/10.1016/S0031-6865(99)00063-1).
- 12 [21] Prajapati VD, Mashru KH, Solanki et al. Development of modified release gliclazide biological
13 macromolecules using natural biodegradable polymers. *Int. J. Biol. Macromol.* 2013, 55: 6-14. doi:
14 <http://dx.doi.org/10.1016/j.ijbiomac.2012.12.033>.
- 15 [22] Varshosaz J, Talari R, Mostafavi S et al. Dissolution enhancement of gliclazide using in situ
16 micronization by solvent change method. *Powder Technol*, 2008, 187: 222-230. doi:
17 <http://dx.doi.org/10.1016/j.powtec.2008.02.018>.
- 18 [23] Rivas C, Tarhinia M, Badria W et al. Nanoprecipitation process: From encapsulation to drug
19 delivery. *Int. J. Pharm.* 2017, 532: 66–81.
- 20 [24] Fangueiro JF, Andreani T, Egea M et al. Experimental factorial design applied to mucoadhesive
21 lipid nanoparticles via multiple emulsion process. *Colloids and Surfaces B: Biointerfaces*, 2012, 100:
22 84-89. doi: <http://dx.doi.org/10.1016/j.colsurfb.2012.04.014>.
- 23 [25] Chang J, Lee Y, Wang Y. Optimization of Nanosized Silver Particle Synthesis via Experimental
24 Design. *Ind. Eng. Chem. Res.* 2007, 46: 5591-5599.
- 25 [26] Jain A, Jain S, Ganesh N. et al. Design and development of ligand-appended polysaccharidic
26 nanoparticles for the delivery of oxaliplatin in colorectal cancer. 2010. *Nanomedicine:*
27 *Nanotechnology, Biology and Medicine*, 2010, 6: 179-190. doi:
28 <http://dx.doi.org/10.1016/j.nano.2009.03.002>.
- 29 [27] Averineni R, Shavi G, Ranjan O. et al. Formulation of Gliclazide Encapsulated Chitosan
30 Nanoparticles: In Vitro and In Vivo Evaluation. In: *Anonymous Nano Formulation*, 2012. The Royal
31 Society of Chemistry. 2012, 77-85.
- 32 [28] Obeidat W, Price J. Preparation and evaluation of Eudragit S 100 microspheres as pH-sensitive
33 release preparations for piroxicam and theophylline using the emulsion-solvent evaporation method.
34 *J Microencapsul.*, 2006, 23: 195-202. doi: 10.1080/02652040500435337
- 35 [29] Thomas, R., Moon, M., Lee, S., Jeong, Y. Paclitaxel loaded hyaluronic acid nanoparticles for
36 targeted cancer therapy: In vitro and in vivo analysis. *Int. J. Biol. Macromole.* 2015, 72, 510-518.
- 37 [30] Wittaya-areekul S, Krueenate J, Prahsarn C. Preparation and in Vitro Evaluation of Mucoadhesive
38 Properties of alginate/chitosan Microparticles Containing Prednisolone. *Int. J. Pharm.* 2006, 312: 113–
39 118.
- 40 [31] Borges O, Cordeiro-da-Silva A, Romeijn, S. et al. Uptake studies in rat Peyer's patches,
41 cytotoxicity and release studies of alginate coated chitosan nanoparticles for mucosal vaccination. *J.*
42 *Control. Rel.* 2006, 114: 348–358.
- 43 [32] Zhang Y, Wei W, Lv P. et al. Preparation and evaluation of alginate–chitosan microspheres for
44 oral delivery of insulin. *Eur. J. Pharm. Biopharm.* 2011, 77: 11-19.
- 45
46
47
48
49
50
51
52
53
54
55
56
57
58
59
60
61
62
63
64
65

1 [33] Chaves P, Frank L, Frank A. et al. Mucoadhesive Properties of Eudragit®RS100, Eudragit®S100,
2 and Poly(ε-caprolactone) Nanocapsules: Influence of the Vehicle and the Mucosal Surface. AAPS
3 PharmSciTech, 2018, 19 (No 4): 1637-1646.

4 [34] Otagiri O, Imai T, Hirayama F. et al. Inclusion complex formations of the antiinflammatory drug
5 flurbiprofen with cyclodextrins in aqueous solution and in solid state. Acta Pharm. Suec., 1983, 20:
6 11–20.

7 [35] Pignatello R, Ferro M, Puglisi G. Preparation of solid dispersions of nonsteroidal anti-
8 inflammatory drugs with acrylic polymers and studies on mechanisms of drug-polymer interactions.
9 AAPS Pharm. Sci. Tech., 2002, 3(2): 35–45.

10 [36] Bari A., Chella N, Sanka K. et al. Improved anti-diabetic activity of glibenclamide using oral self
11 nano emulsifying powder. J Microencapsul. 2015, 32(1): 54–60.

12 [37] Guo S, Wang G, Wu T. et al. Solid dispersion of berberine hydrochloride and Eudragit® S100:
13 Formulation, physicochemical characterization and cytotoxicity evaluation. J. Drug Del. Sci. Techno.
14 2017, 40: 21-27.

15 [38] Mohd A, Sanka K, Bandi S. et al. Solid self-nanoemulsifying drug delivery system (S-SNEDDS)
16 for oral delivery of glimepiride: development and antidiabetic activity in albino rabbits. Drug Deliv.
17 2015, 22(4): 499–508.

18 [39] Hu D, Liu L, Chen W. et al. A novel preparation method for 5-aminosalicylic acid loaded Eudragit
19 S100 nanoparticles. Int. J. Mol. Sci. 2012, 13: 6454-6468; doi:10.3390/ijms13056454.

20 [40] Costa P, Lobo S. Modeling and comparison of dissolution profiles. Eur. J. Pharm. Sci. 2001,
21 13(2): 123-133.

22 [41] Proks P, Reimann F, Green N. et al. Sulfonylurea Stimulation of Insulin Secretion. Diabetes,
23 2002, 51(3): S368-S376. http://diabetes.diabetesjournals.org/content/51/suppl_3/S368.

24 [42] Behzadi S, Serpooshan, V, Tao W, Hamaly M, , Alkawareek M et al. Cellular Uptake of
25 Nanoparticles: Journey Inside the Cell. Chem Soc Rev. 2017,17; 46(14): 4218–4244.

26 [43] Snejdrova, E, Dittrich, M. Pharmaceutical Applications of Plasticized Polymers, Recent
27 Advances in Plasticizers, 2012. Dr. Mohammad Luqman (Ed.), ISBN: 978-953-51-0363-9, InTech,
28 Available from: [http://www.intechopen.com/books/recent-advances-in-plasticizers/pharmaceutical-
29 applications-of-plasticized](http://www.intechopen.com/books/recent-advances-in-plasticizers/pharmaceutical-applications-of-plasticized-polymers) polymers.

30
31
32
33
34
35
36
37
38
39
40
41
42
43
44
45
46
47
48
49
50
51
52
53
54
55
56
57
58
59
60
61
62
63
64
65

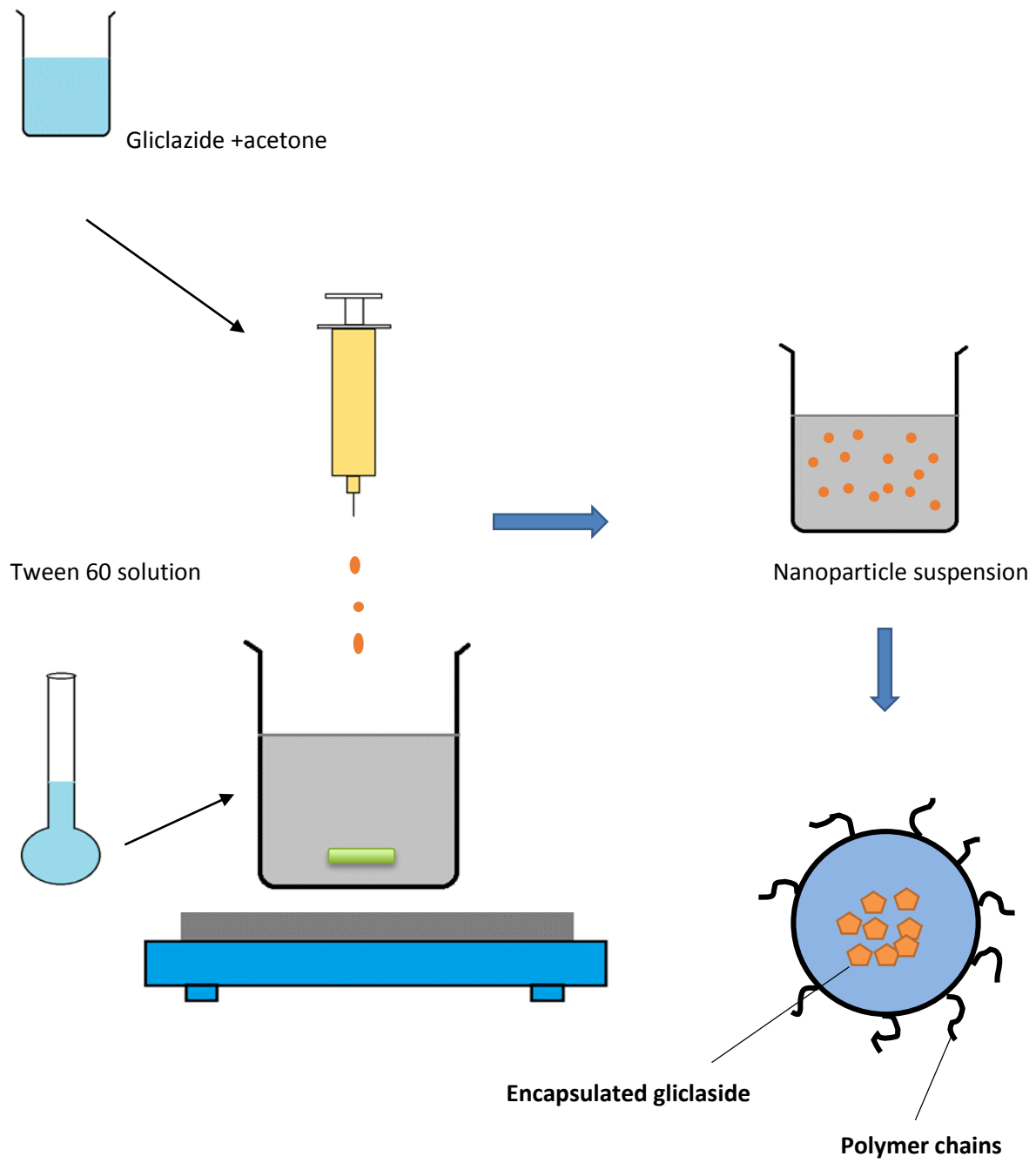
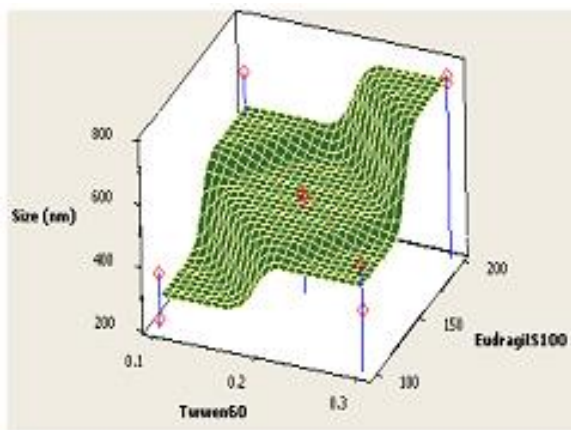
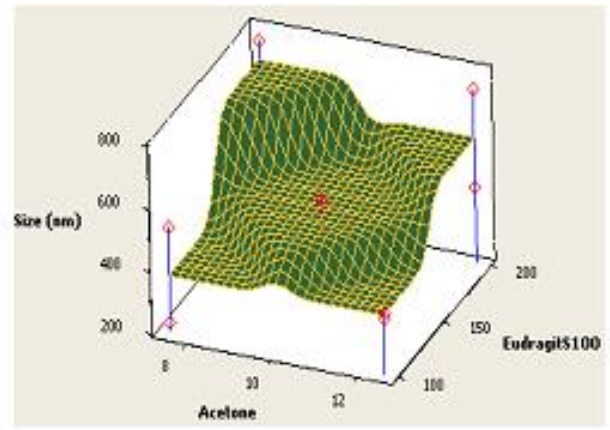


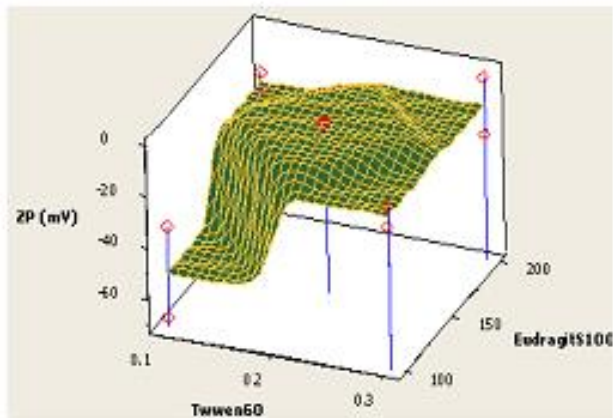
Figure 1: Representation of pH sensitive gliclazide nanoparticles preparation using nanoprecipitation technique



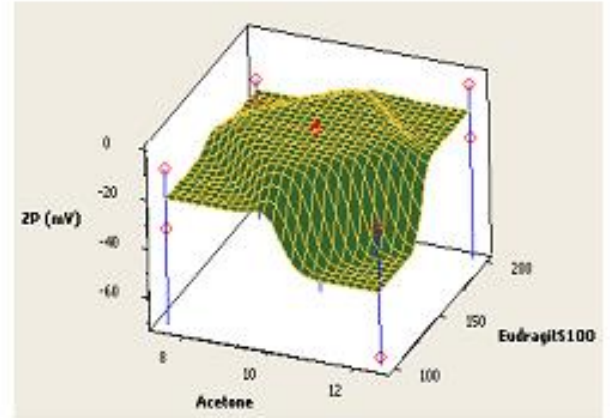
A



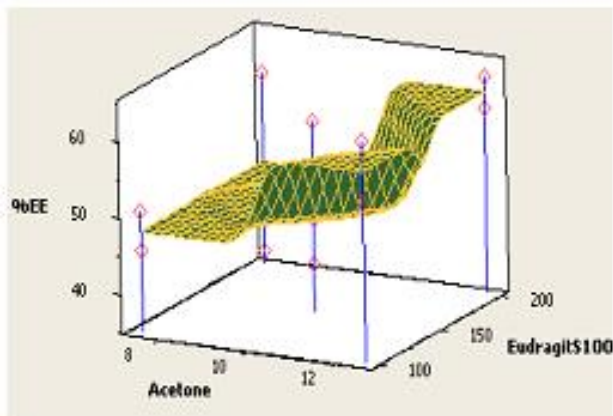
B



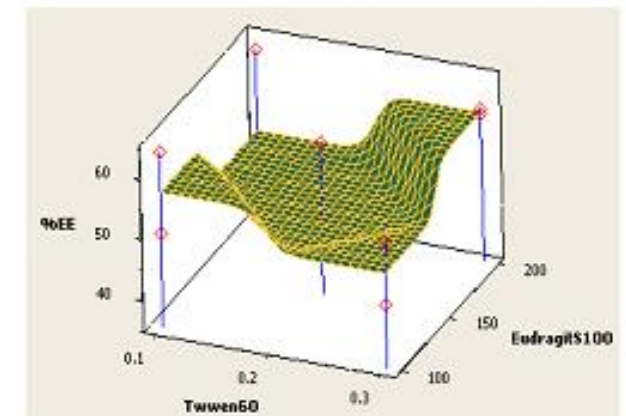
C



D



E



F

Figure 2: Surface responses plots showing the effects of formulation variables on size (A-B), ZP (C-D) and entrapment efficiency (E-F).

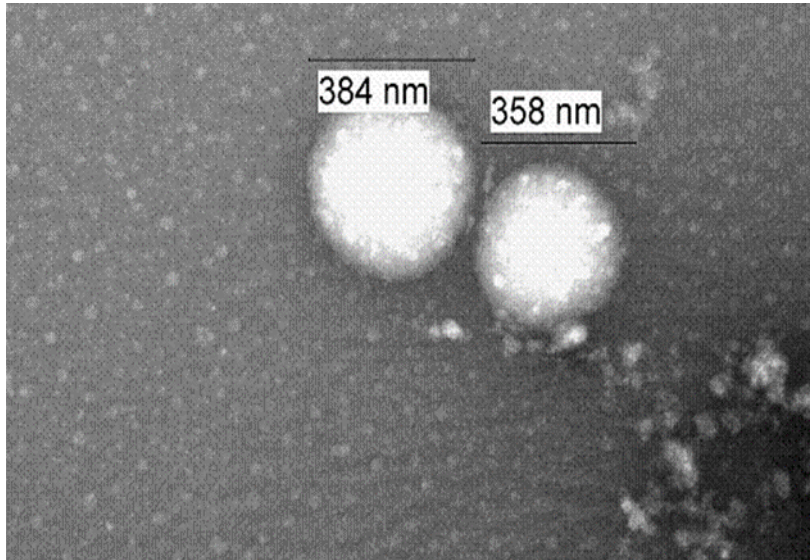


Figure 3: TEM images of gliclazide-loaded Eudragit nanoparticles

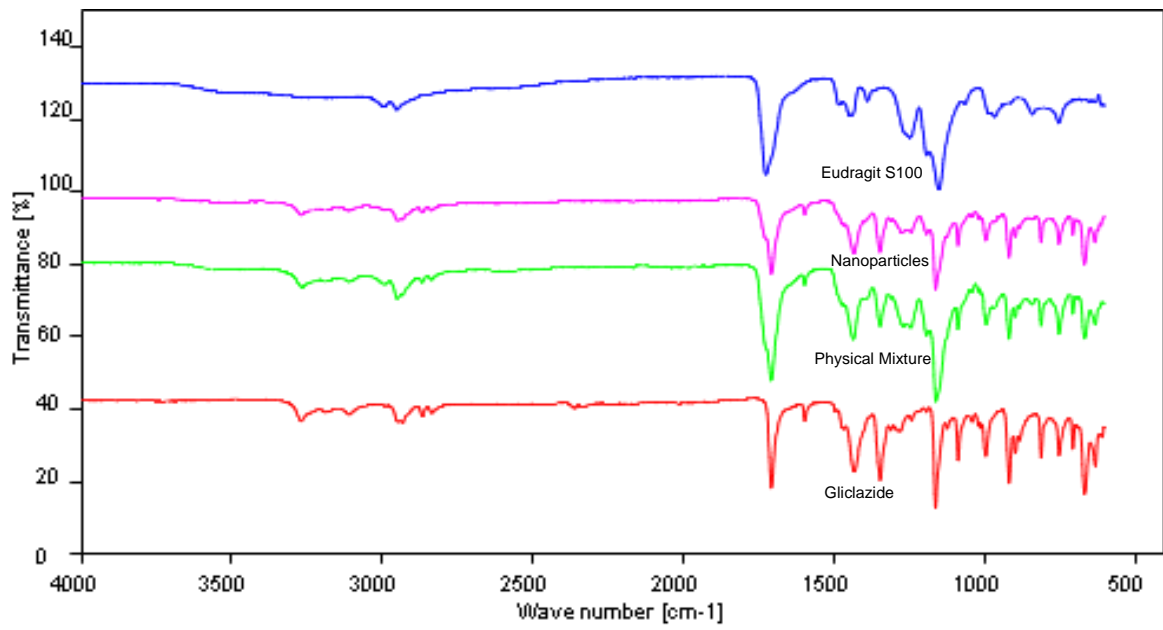


Figure 4: FTIR spectra of pure gliclazide, Eudragit® S100, gliclazide loaded Eudragit nanoparticles and 1:1 physical mixture of Eudragit S®100 polymer and gliclazide.

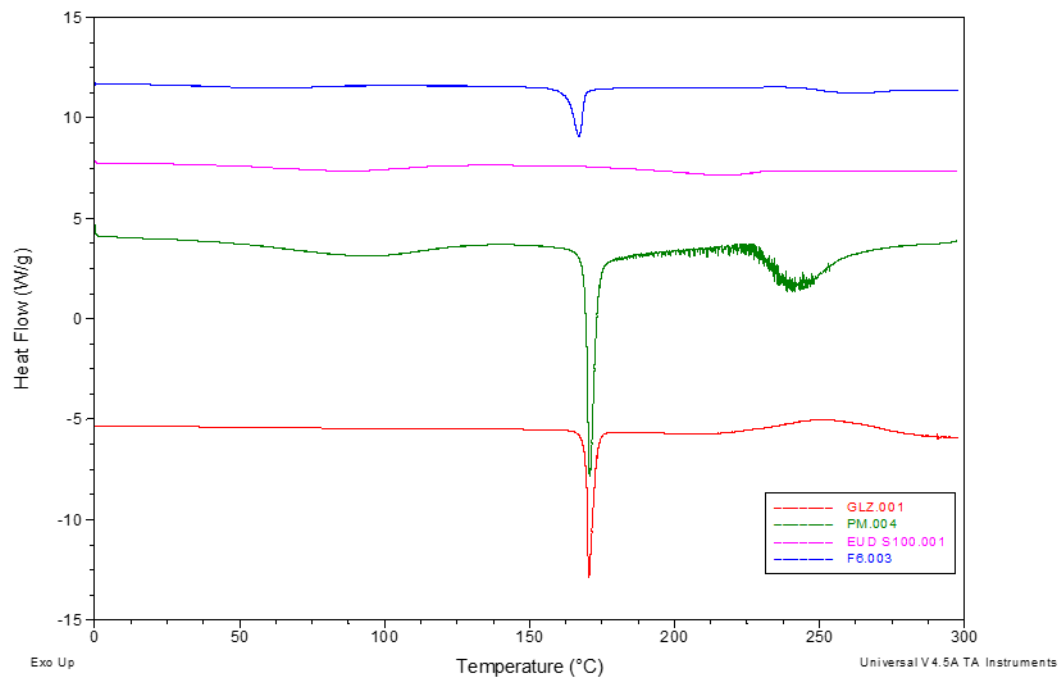


Figure 5: DSC graph of pure GLZ, Eudragit® S100, gliclazide loaded Eudragit nanoparticles represented by (F6) and 1:1 Physical Mixture of gliclazide and Eudragit® S100.

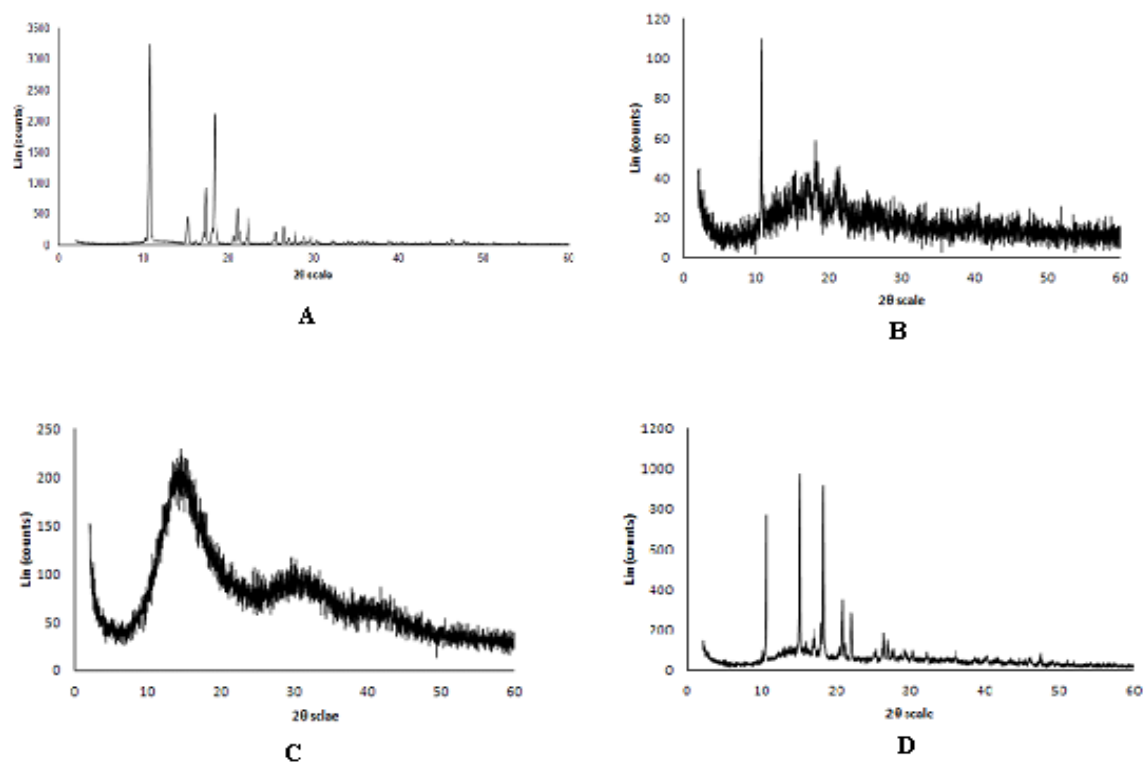


Figure 6: XRD spectra of pure GLZ (A), Eudragit® S100 (B), gliclazide-loaded Eudragit nanoparticles (C) and 1:1 Physical Mixture of gliclazide and Eudragit® S100 (D).

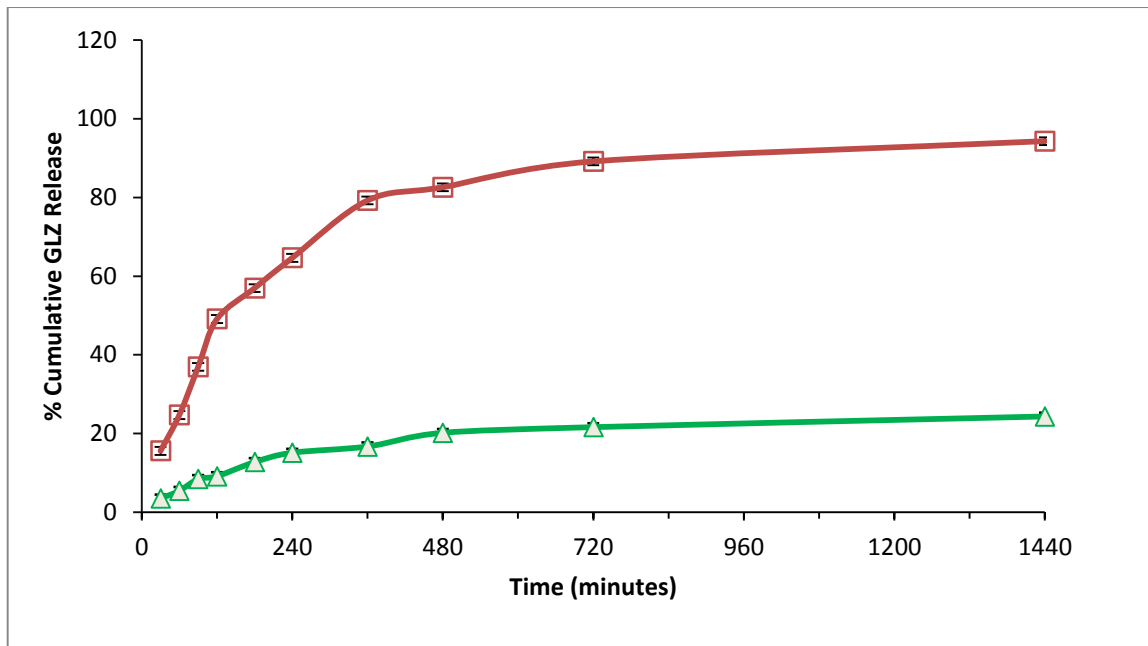
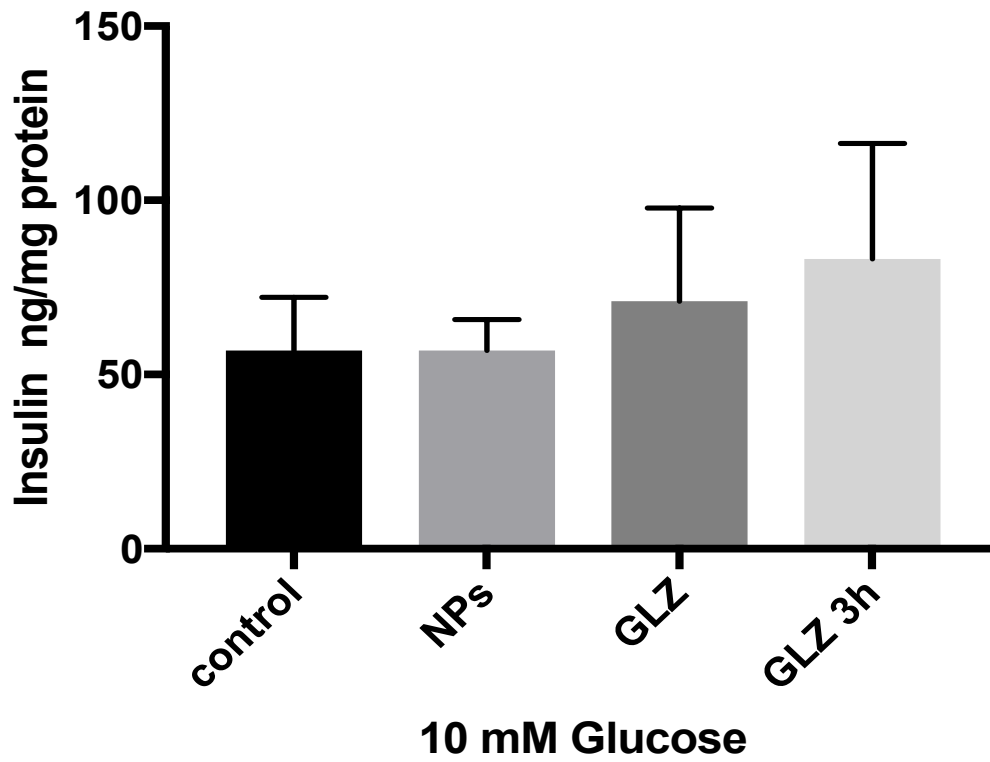
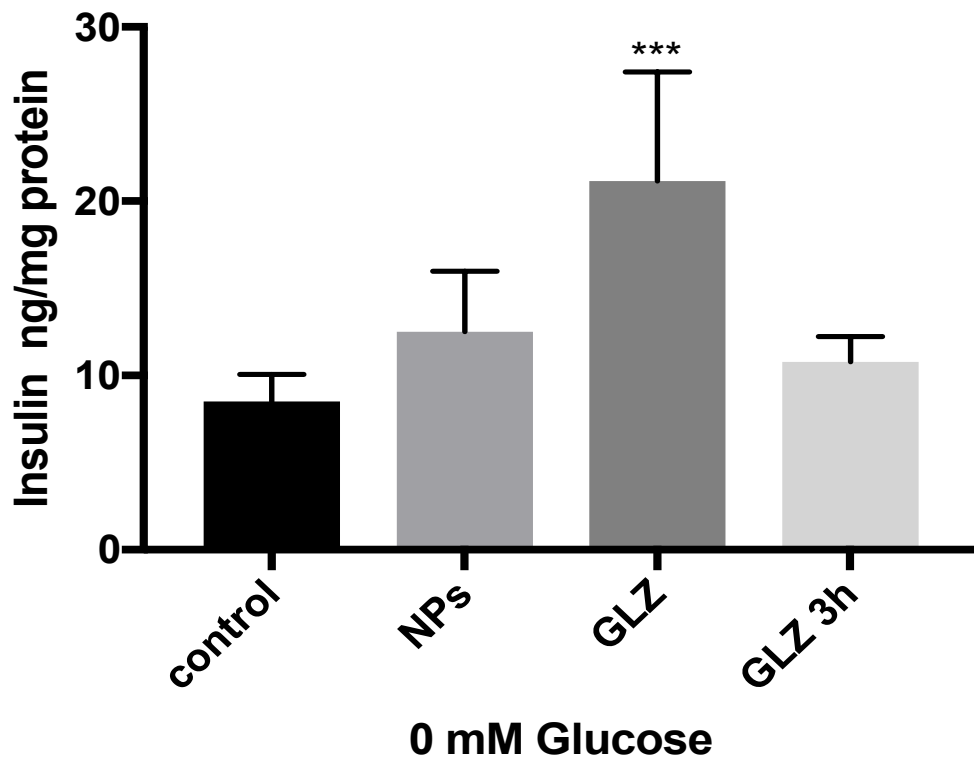


Figure 7: *In-vitro* release studies of GLZ NPs in phosphate buffer pH 7.2 and 0.1 M HCl.
pH 7.4 ■ , 0.1 M HCl ▲



Figures 8 a&b: Gliclazide loaded Eudragit nanoparticles increased insulin secretion in BTC F7 cells

Table-1: Initial 3 level factorial design, providing the lower, medium and upper level values for each variable.

Variables	Levels		
	Low level (-1)	Medium Level (0)	High level (+1)
Eudragit S-100 (mg) X₁	100	150	200
Tween 60 (%)X₂	0.1	0.2	0.3
Acetone (ml) X₃	7.5	10	12.5

Table-2: Response values of size, zeta potential and entrapment efficiency of three factor depicted in table 1 for the 11 experiment formulations

Run	Eudragit S-100	Tween 60 (%wt)	Acetone (ml)	(Size)		ZP (mV)		%EE	
	X ₁	X ₂	X ₃	Mean	SD	Mean	SD	Mean	SD
1	200	0.1	7.5	641.933	13.336	-16.267	1.159	44.216	7.230
2	100	0.1	7.5	222.233	5.590	-33.200	1.114	51.089	0.441
3	200	0.3	7.5	579.200	166.679	-24.100	0.985	60.787	0.902
4	100	0.3	7.5	530.000	33.899	-8.847	0.060	46.422	3.606
5	200	0.1	12.5	615.867	182.801	-21.733	2.914	59.173	5.969
6	100	0.1	12.5	364.033	5.750	-29.100	1.931	57.461	5.602
7	200	0.3	12.5	883.600	539.745	-1.239	0.865	54.895	3.987
8	100	0.3	12.5	340.267	43.506	-19.633	2.548	51.922	3.833
9	150	0.2	10	471.733	14.851	-5.760	0.449	43.478	2.440
10	150	0.2	10	508.767	8.784	-6.437	0.159	46.311	11.788
11	150	0.2	10	494.833	9.432	-5.667	0.484	44.755	3.346

Table-3: Analysis of mean particle size (Z-Ave) by ANOVA statistical test

Source	Sum of Squares	df	Mean Square	F-value	p-value
EudragitS100	599199.202	1	599199.202	20.127	.000153
Tween 60	89670.375	1	89670.375	3.012	.095471
Acetone	19906.560	1	19906.560	.669	.421559
X₁ X₂	2340.375	1	2340.375	.079	.781586
X₁ X₃	39918.727	1	39918.727	1.341	.258271
X₂ X₃	.427	1	.427	.0000143	.997011
Error	714485.949	4	29770.248		
Total	1465522	10			

Table-4: Analysis of zeta potential (ZP) by ANOVA statistical test

Source	Sum of Squares	df	Mean Square	F-value	p-value
EudragitS100	1705.608	1	1705.608	852.324	.000000
Tween 60	2804.611	1	2804.611	1401.516	.000000
Acetone	321.765	1	321.765	160.792	.000000
X₁ X₂	1402.659	1	1402.659	700.935	.000000
X₁ X₃	1539.890	1	1539.890	769.512	.000000
X₂ X₃	1070.978	1	1070.978	535.187	.000000
Error	48.027	4	2.001		
Total	8894	10			

Table-5: Analysis of entrapment efficiency by ANOVA statistical test

Source	Sum of Squares	df	Mean Square	F-value	p-value
EudragitS100	55.608	1	55.608	2.047	.1654160
Tween 60	1.633	1	1.633	.060	.8084202
Acetone	164.400	1	164.400	6.051	.0214814
X₁ X₂	189.810	1	189.810	6.987	.0142385
X₁ X₃	2.954	1	2.954	.109	.7444529
X₂ X₃	176.909	1	176.909	6.512	.0175050
Error	652.027	4	27.168		
Total	1243	10			